Asian Journal of Chemistry Vol. 20, No. 6 (2008), 4595-4608

3D-QSAR Studies of Imidazole Derivatives as *Candida albicans* P450 - Demethylase Inhibitors

SWASTIKA GANGULY* and S. BANERJEE
Department of Pharmaceutical Sciences, Birla Institute of Technology Mesra, Ranchi-835 215, India.
E-mail: pompi123@rediffmail.com

In present search for better antifungal agents with high degree of specificity towards fungal enzymes, 3D-QSAR studies of some antifungal imidazoles was performed by comparative molecular field analysis (CoMFA) and comparative molecular similarity indices analysis (CoMSIA) methods. The compounds were divided into a training set of 34 molecules and a test set of 15 molecules. The global minimum energy conformer of the template molecule miconazole, **1** was obtained by simulated annealing method and used to build the structures of the molecules in the dataset. Tripos's Sybyl 7.1 program was used to develop the 3D CoMFA and CoMSIA models. The CoMFA model produced statistically significant results with cross-validated and conventional correlation coefficients of 0.697 and 0.925, respectively. The combination of steric, electrostatic, hydrophobic and hydrogen acceptor fields in CoMSIA gave results with cross-validated and conventional correlation coefficients of 0.656 and 0.912, respectively. The predictive ability of CoMFA and CoMSIA were determined using a test set of 15 imidazole derivatives giving predictive correlation coefficients of 0.66 and 0.57, respectively indicating good predictive power of CoMFA over CoMSIA. Based upon the information derived from CoMFA and CoMSIA, newer imidazole derivatives can be designed as potent *Candida* $P450_{DM}$ inhibitors.

Key Words: 1-Substituted 2-methylimidazoles, CoMFA, CoMSIA.

INTRODUCTION

During the last 30 years, a number of antifungal agents[1,2] containing the imidazole nucleus have been introduced. Differential inhibition of cytochrome P-450 dependent lanosterol 14 α-demethylase ($P\text{-}450_{DM}$) between pathogenic fungi and man is the basis for clinically important activity of azole antifungal agents and the specificity of the inhibitors is determined by the differential complementarity between the structure of the agent and the active sites of the fungal and the host enzymes[3]. One of the reasons to

continue the search for better antifungal agents is to increase the specificity toward fungal enzymes. This is particularly important under pathological circumstances where the immune system is compromised to a great extent (AIDS pathology, major surgery interventions) and the side effects (inhibition of host P-450$_{DM}$) due to over dosage of the azole compounds which may eventually cause death of the patients[3]. Although P-450$_{DM}$ enzymes have been purified from different sources[4-7], no experimental structural information on the active site of the target enzyme *Candida* P450$_{DM}$ is available. In such circumstances, the indirect approach *i.e.* ligand based approaches like 3D-QSAR studies are quite useful for lead optimization and drug design. Since its introduction in 1988, CoMFA[8] has rapidly become one of the most powerful tools for 3D-QSAR studies[9-11]. CoMFA methodology is based on the assumption that the changes in the biological activity correlate with the changes in the steric and electrostatic fields of the molecules[11]. The CoMSIA[12] method differs by the way the molecular fields are calculated and by including additional molecular fields, such as lipophilic and hydrogen bond potential. The additional fields in CoMSIA provide better visualization and interpre-tation of the obtained correlation in terms of field contribution to the activity of the compound[11].

In this study, a comparative molecular field analysis (CoMFA) and comparative molecular similarity indices analysis (CoMSIA) using SYBYL 7.1[13] was carried out on a series of 1-substituted imidazole analogs[14,15] (Tables 1 and 2) to obtain a robust 3D QSAR model with significant cross validated correlation coefficient and predictive r^2 value which would be well able to explain and predict the activity of novel imidazole analogs active against *Candida albicans* P-450$_{DM}$ and will be helpful in design of new and more selective antifungals.

EXPERIMENTAL

A series of 1-substituted imidazole ethers (**1-29**) (Table-1) and 1-(2-alkyl-2-phenylethyl)-1*H*-imidazoles (**30-49**) (Table-2) were taken for the QSAR study. The biological activity data of various imidazoles was obtained from Heeres *et al.*[14,15]. A series of 49 molecules were taken for the study. The compounds were divided into a training set of 34 molecules and test set of 15 molecules. All the molecular modeling techniques *viz.*, CoMFA, CoMSIA studies were performed using the SYBYL (version 7.1) software installed in a Dell system (3.4 GHz Processor, 512 MB RAM, 80 GB Hard Disk) with Red Hat Linux Enterprise version 3.0 as the operating system. An essential requirement for 3D-QSAR techniques using molecular field analysis is knowledge of the active conformation of agonist or antagonist under study. Since the crystal structure of cytochrome P-450$_{DM}$ of *Candida albicans* is not available, the least energy conformer was used as the bioactive

TABLE-1
DATASET OF 1-SUBSTITUTED IMIDAZOLE ETHERS
USED FOR 3D-QSAR ANALYSES

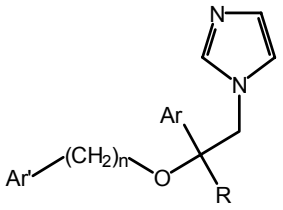

Compd. no.	n	R	Ar	Ar′	MIC	-log MIC
1	1	H	2,4-Cl_2- C_6H_3	2,4-Cl_2- C_6H_3	10	1.00
2	1	H	5-Cl-2-thienyl	*o*-Cl-C_6H_4	100	2.00
3	1	H	*p*-F- C_6H_4	*p*-Cl- C_6H_4	100	2.00
4	1	H	*p*-F- C_6H_4	*o*-Cl- C_6H_4	100	2.00
5	1	H	C_6H_4	*p*-Cl- C_6H_4	100	2.00
6	1	H	*o*- CH_3 - C_6H_4	2,4-Cl_2- C_6H_3	100	2.00
7	1	CH_3	*p*-Cl- C_6H_4	*p*-Cl- C_6H_4	100	2.00
8	1	H	*o*- CH_3 - C_6H_4	2,4-Cl_2- C_6H_3	100	2.00
9	1	H	2,4-Cl_2- C_6H_3	*m*-CH_3O- C_6H_4	100	2.00
10	1	H	*p*-Cl- C_6H_4	*o*- CH_3 - C_6H_4	100	2.00
11	1	CH_3	C_6H_4	*p*-Cl- C_6H_4	100	2.00
12	1	H	*p*- CH_3 - C_6H_4	*p*-Cl- C_6H_4	100	2.00
13	1	H	1*m*-$C(CH_3)_2CHC_6H_5OCH_2$	C_6H_4-*p*-Cl	100	2.00
14	1	H	2,4-Cl_2- C_6H_3	2,6-Cl_2- C_6H_3	100	2.00
15	1	H	2,4-Cl_2- C_6H_3	*p*-F- C_6H_4	100	2.00
16	1	H	2,4-Cl_2- C_6H_3	*o*-Cl-C_6H_4	100	1.00
17	1	H	2,4-Cl_2- C_6H_3	*p*-Cl- C_6H_4	100	2.00
18	1	H	*p*-Cl- C_6H_4	2,4-Cl_2- C_6H_3	100	1.00
19	0	H	*p*-Br- C_6H_4	*o*-Cl- C_6H_4	100	2.00
20	1	H	2,4-Cl_2- C_6H_3	2,4-Cl_2- C_6H_3	10	1.00
21[a]	0	H	2,4-Cl_2- C_6H_3	*p*-NO_2- C_6H_4	100	2.00
22[a]	1	H	*p*-F- C_6H_4	2,4-Cl_2- C_6H_3	100	2.00
23[a]	1	H	2,4-Cl_2- C_6H_3	*o*-F- C_6H_4	100	2.00
24[a]	1	H	*o*-Cl- C_6H_4	2,4-Cl_2- C_6H_3	100	2.00
25[a]	1	H	*o*-Cl- C_6H_4	*o*-Cl- C_6H_4	100	2.00
26[a]	1	H	*o*-Cl- C_6H_4	*p*-Cl- C_6H_4	100	2.00
27[a]	1	H	*p*- CH_3 - C_6H_4	2,4-Cl_2- C_6H_3	100	2.00
28[a]	1	H	2,4-Cl_2- C_6H_3	*o*- CH_3 - C_6H_4	100	2.00
29[a]	1	H	2,4-Cl_2- C_6H_3	*p*- CH_3O- C_6H_4	100	2.00
30[a]	0	H	*p*- CH_3 - C_6H_4	*o*-Cl- C_6H_4	100	2.00

[a]Test set compounds.

TABLE-2
DATASET OF 1-(2-ALKYL-2-PHENYLETHYL)-
1*H*-IMIDAZOLES USED FOR 3D-QSAR ANALYSES

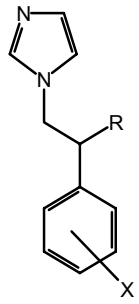

Compd. No.	X	R	MIC	-log MIC
31	4-F	*n*-C_7H_{15}	10.00	1.00
32	4-F	*n*-C_8H_{17}	10.00	1.00
33	4-Cl	*n*-C_6H_{13}	100.00	2.00
34	4-Cl	*n*-C_8H_{17}	10.00	1.00
35	4-Br	*n*-C_6H_{13}	10.00	1.00
36	4-Br	*n*-C_7H_{15}	10.00	1.00
37	2,4-Cl	*i*-C_5H_{11}	10.00	1.00
38	2,4-Cl	*n*-C_6H_{13}	10.00	1.00
39	2,4-Cl	*n*-C_7H_{15}	10.00	1.00
40	2,4-Cl	*n*-C_8H_{17}	10.00	1.00
41	2,6-Cl	*n*-C_5H_{11}	10.00	1.00
42	2,6-Cl	*n*-C_7H_{15}	10.00	1.00
43	2-Cl	*n*-C_7H_{15}	10.00	1.00
44	2-Br	*n*-C_6H_{13}	10.00	1.00
45[a]	2-Br	*n*-C_4H_9	100.00	2.00
46[a]	4-F	*n*-C_6H_{13}	100.00	2.00
47[a]	4-Cl	*n*-C_5H_{11}	100.00	2.00
48[a]	4-Br	*n*-C_4H_9	100.00	2.00
49[a]	2,4-Cl_2	*i*-C_4H_9	100.00	2.00

[a]Test set compounds.

conformation. The initial conformation of the reference standard miconazole **1** was obtained from simulated annealing as it enables the rapid identification of the global minimum energy conformer[16]. The system was subjected to simulated annealing by heating at 700 K for 1000 fs and then cooling at 200 K for 1000 fs. The exponential annealing function was used and 10 such cycles were run. The least energy conformer obtained by this method was subjected to further minimization. The minimized conformer, thus obtained, was taken as the template and rest of the molecules were built

from it. A constrained minimization followed by full minimization was carried out on these molecules in order to prevent the conformations moving to a false region[11]. Tripos force field was used and partial charges were calcu-lated using Gasteiger-Huckel method. Powell's conjugate gradient method was used for minimization. The gradient of 0.01 kcal mol^{-1} $Å^{-1}$ was set as a convergence criterion. In CoMFA studies alignment of molecule is one of the most sensitive input areas[11]. The reference standard miconazole **1** was taken and the rest of the molecules were aligned to it using the Data-base Alignment method in the SYBYL. The molecules were aligned to the template molecule by using common substructure labeled with * in **1** (Fig. 1). The aligned molecules are shown in Fig. 2.

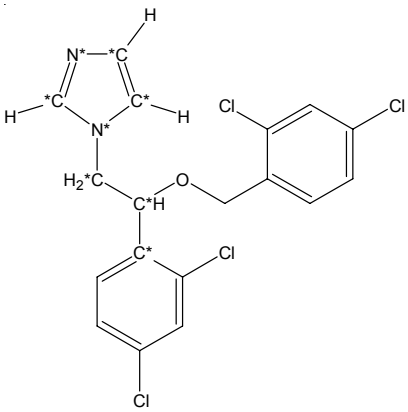

Fig. 1. Structure of miconazole (**1**)

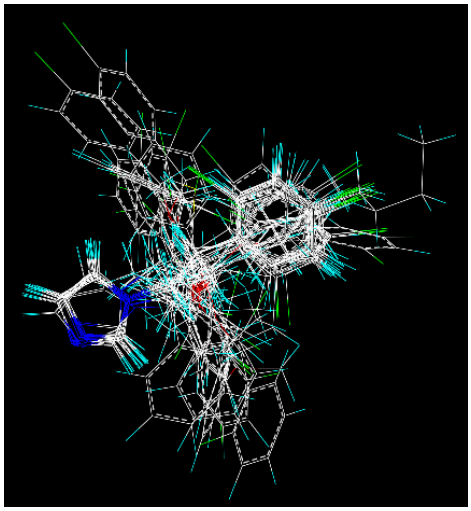

Fig. 2. Alignment of the training set molecules

CoMFA interaction energy calculation[11]: The steric and electrostatic CoMFA fields were calculated at each lattice intersection of a regularly spaced grid of 2.0 Å in all three dimensions within defined region. The van der Waals potential and coulombic term representing the steric and electrostatic fields, respectively were calculated using standard Tripos force fields. A distance-dependent dielectric constant of 1.00 was used. An sp^3 carbon atom with + 1.00 charge was used as a probe atom. The steric and electrostatic fields were truncated at + 30.00 kcal mol^{-1} and the electrostatic fields were ignored at the lattice points with maximal steric interactions.

CoMSIA interaction energy calculation[11]: The steric, electrostatic, hydrophobic, hydrogen bond donor and hydrogen bond acceptor potential fields were calculated at each lattice intersection of a regularly spaced grid of 2.0 Å. A probe atom with radius 1.0 Å and + 1.0 charge with hydrophobicity of + 1.0 and hydrogen bond donor and hydrogen bond acceptor properties of + 1.0 was used to calculate steric, electrostatic, hydrophobic, donor and acceptor fields. The contribution from these descriptors was truncated at 0.3 kcal mol^{-1}.

Partial least square analysis (PLS)[11]: PLS method was used to linearly correlate the CoMFA fields to the minimum inhibitory concentrations of the compounds. The cross-validation[17,18] analysis was performed using the leave one out (LOO) method in which one compound is removed from the dataset and its activity is predicted using the model derived from the rest of the dataset. The cross-validated r^2 that resulted in optimum number of components and lowest standard error of prediction were considered for further analysis. Equal weights were assigned to steric and electrostatic fields using CoMFA_STD scaling option. To speed up the analysis and reduce noise, a minimum filter values of 2 kcal mol^{-1} was used. Final analysis was performed to calculate conventional r^2 using the optimum number of components. The entire cross-validated results were considering the fact[19] that a value of r^2_{cv} above 0.3 indicates that probability of chance correlation is less than 5 %.

Predictive correlation coefficient[11]: The predictive ability of each 3D-QSAR model was determined from a set of seven compounds that were not included in the training set. These molecules were aligned and their activities were predicted. The predictive correlation coefficient (r^2_{pred}), based on molecules of test set, is defined as,

$$r^2_{pred} = (SD\text{-}PRESS)/SD$$

where SD is the sum of the squared deviations between the biological activities of the test set and mean activities of the training set molecules and PRESS is the sum of squared deviation between predicted and actual activity values for every molecule in test set.

RESULTS AND DISCUSSION

The CoMFA model obtained with 34 imidazole derivatives in training set resulted in a five-component model with cross-validated correlation coefficient of 0.697 and minimum standard error. This analysis was used for final non-cross validated run, giving a correlation coefficient of 0.925 giving a good linear correlation between the observed and predicted activities of the molecules in the training set. To test the predictive ability of the resulting model, a test set of 15 molecules excluded from the model creation work was used. The predictive correlation coefficient of 0.66 was obtained for CoMFA model. Table-3 shows the results of PLS analysis for CoMFA and CoMSIA. The alignment of the training set molecules is shown in Fig. 2. The relative contributions of steric and electrostatic fields for CoMFA are in the ratio 7:3 (Table-3). Steric interactions of molecule with active site of the enzyme could be an important factor for cytochrome P-450_{DM} inhibitory activity. A plot of predicted (CoMFA) *versus* actual activity for training set molecules is shown in Fig. 3, while Fig. 4 represents the plot of predicted (CoMSIA) *versus* actual activity values. The test set residuals of CoMFA and CoMSIA analyses are shown in Fig. 5. The actual, predicted and residual values of training and test set of the imidazole analogs for CoMFA and CoMSIA are given in Tables 4 and 5, respectively. Contour maps were generated as scalar product of coefficients and standard deviation associated with each CoMFA column. The 3D-QSAR contour maps revealing the contribution of CoMFA and CoMSIA fields are shown in Figs. 6-8, respectively. The CoMFA steric interactions are represented by green (G) and yellow (Y) contours while electrostatic interactions are represented by red (R) and blue (B) contours. The bulky substituents are favoured in green (G) regions and disfavoured in yellow (Y) regions. The increase in positive charge is favoured in blue (B) regions while the increase in negative charge is favoured in red (R) regions. One of the most active molecules **2** is displayed in the background of contours. The steric contours (Fig. 6a) show a green (G) contour near the *p*-position of the phenyl ring of the template molecule where bulky substituents are expected to increase the activity. Introduction of bulky group on the 2nd position of the imidazole ring is also sterically favoured as shown by the green (G) contour. The steric contours also show a yellow (Y) contour near the 4th position of the imidazole nucleus. Hence, this position should always be sterically unhindered for good antifungal activity. The electrostatic contours of CoMFA (Fig. 6b) show a blue (B) contour around the thienyl group of the template molecule where low electron density is expected to increase the activity. The electrostatic contours also show a red (R) contour near the ethereal linkage C-O-C where high electron density is expected to increase the activity.

TABLE-3
SUMMARY OF CoMFA AND CoMSIA STATISTICS

Parameters	CoMFA	CoMSIIA
r^2_{cv}	0.697	0.656
n	5.000	5.000
r^2	0.925	0.912
SEE	0.150	0.165
F-test value	68.830	46.728
PRESS	0.385	0.492
r^2_{pred}	0.660	0.570
SD	1.150	1.150
Contributions (%)		
Steric	0.695	0.173
Electrostatic	0.305	0.171
Hydrophobic	–	0.414
Acceptor	–	0.242

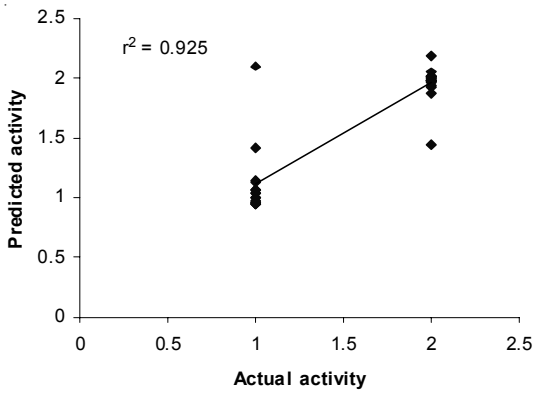

Fig. 3. Plot of predicted *versus* actual -log MIC values of training set molecules for CoMFA model.

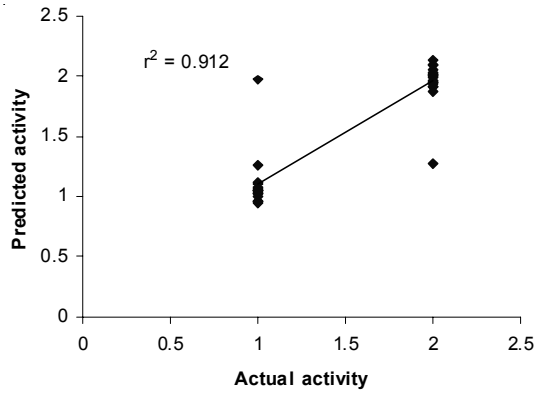

Fig. 4. Plot of predicted *versus* actual -log MIC values of training set molecules for CoMSIA model.

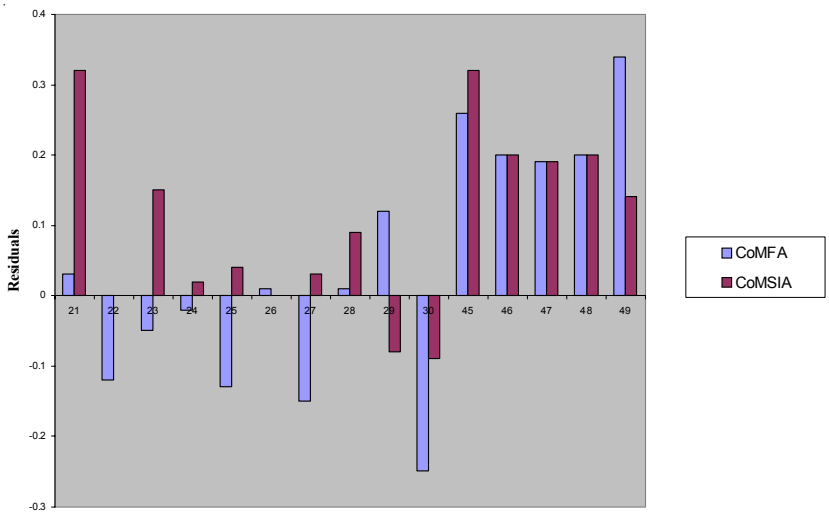

Fig. 5. Histogram of test set molecules

TABLE-4
ACTUAL, PREDICTED INHIBITORY ACTIVITIES (-log MIC)
AND RESIDUALS OF THE TRAINING SET MOLECULES

Compd. no.	Actual -log MIC	Predicted -log MIC		Residuals	
		CoMFA	CoMSIA	CoMFA	CoMSIA
1	1.00	0.95	0.95	0.05	0.05
2	2.00	2.01	2.10	-0.01	-0.10
3	2.00	1.96	1.96	0.04	0.04
4	2.00	2.19	2.09	-0.19	-0.09
5	2.00	2.01	1.87	-0.01	0.13
6	2.00	2.00	2.14	0.00	-0.14
7	2.00	1.97	1.99	0.03	0.01
8	2.00	2.01	2.03	-0.01	-0.03
9	2.00	1.92	1.91	0.08	0.09
10	2.00	1.97	2.00	0.03	0.00
11	2.00	2.05	2.01	-0.05	-0.01
12	2.00	2.00	2.03	0.00	-0.03
13	2.00	1.97	2.03	0.03	-0.03
14	2.00	1.88	1.94	0.12	0.06
15	2.00	1.97	1.91	0.03	0.09
16	2.00	1.98	2.07	0.02	-0.07
17	2.00	1.94	1.96	0.06	0.04
18	1.00	2.09	1.97	-1.09	-0.97
19	2.00	1.97	1.96	0.03	0.04
20	1.00	1.13	1.05	-0.13	-0.05
31	1.00	1.06	1.12	-0.06	-0.12
32	1.00	0.95	1.02	0.05	-0.02

Compd. no.	Actual -log MIC	Predicted -log MIC		Residuals	
		CoMFA	CoMSIA	CoMFA	CoMSIA
33	2.00	1.43	1.28	0.57	0.72
34	1.00	1.04	1.02	-0.04	-0.02
35	1.00	1.42	1.27	-0.42	-0.27
36	1.00	1.14	1.11	-0.14	-0.11
37	1.00	1.04	1.07	-0.04	-0.07
38	1.00	0.96	1.00	0.04	0.00
39	1.00	0.96	0.97	0.04	0.03
40	1.00	1.06	1.06	-0.06	-0.06
41	1.00	1.00	1.05	0.00	-0.05
42	1.00	1.00	0.96	0.00	0.04
43	1.00	0.97	1.05	0.03	-0.05
44	1.00	0.95	1.04	0.05	-0.04

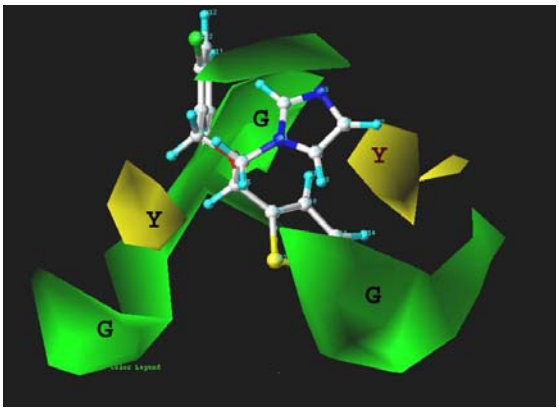

(a)

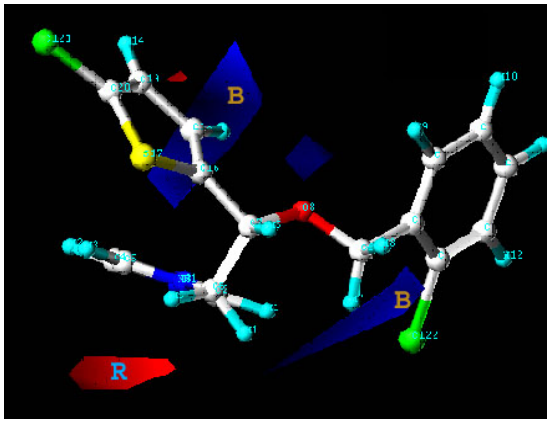

(b)

Fig. 6. The CoMFA steric (a) and electrostatic (b) contour maps. One of the most active molecules **2** is shown in the background. Red (R) is a negative charged region, blue (B) a positively charged region, green (G) a positive sterically active region and yellow (G) a negatively sterically active region

TABLE-5
ACTUAL, PREDICTED INHIBITORY ACTIVITIES (-log MIC)
AND RESIDUALS OF THE TEST SET MOLECULES

Compd. no.	Actual -log MIC	Predicted -log MIC		Residuals	
		CoMFA	CoMSIA	CoMFA	CoMSIA
21	2.00	1.97	1.68	0.03	0.32
22	2.00	2.12	2.00	-0.12	0.00
23	2.00	2.05	1.85	-0.05	0.15
24	2.00	2.02	1.98	-0.02	0.02
25	2.00	2.13	1.96	-0.13	0.04
26	2.00	2.00	1.99	0.01	0.00
27	2.00	2.15	1.97	-0.15	0.03
28	2.00	1.99	1.91	0.01	0.09
29	2.00	2.08	1.88	0.12	-0.08
30	2.00	2.25	2.09	-0.25	-0.09
45	2.00	1.73	1.68	0.26	0.32
46	2.00	1.80	1.80	0.20	0.20
47	2.00	1.81	1.81	0.19	0.19
48	2.00	1.80	1.80	0.20	0.20
49	2.00	1.86	1.66	0.34	0.14

The CoMSIA results were obtained using the same structural alignment and same training and test set as defined in the CoMFA. The combination of steric, electrostatic, hydrophobic and hydrogen acceptor fields in CoMSIA gave a cross-validation correlation coefficient of 0.656, conventional correlation coefficient of 0.912 and predictive correlation coefficient of 0.57. The other combi-nations in CoMSIA gave statistically insignificant results (data not shown). The contributions of steric, electrostatic, hydrophobic and hydrogen acceptor fields are in ratio 2:2:4:2 (Table-3). Comparing this with the field contributions of CoMFA analysis, it is revealed that steric hydrophobic interactions could be an important factor for cytochrome $P450_{DM}$ inhibitory activity. A compar-ison of the residuals of the models from CoMFA and CoMSIA is made to evaluate their predictive ability (Table-5).

Considering the steric contours of CoMSIA (Fig.7a), green (G) contours indicate favourable regions while yellow (Y) contours indicate unfavourable regions for bulkier substituents. In the electrostatic contours of CoMSIA (Fig. 7b), the introduction of electronegative substituents in red (R) regions may increase the affinity while in blue (B) regions decrease the affinity. The steric and electrostatic contours produced by CoMFA (Fig. 6) and CoMSIA (Fig. 7) are similar. In hydrophobic contours, the yellow (Y) regions favour hydrophobic groups while white (W) regions favour hydrophilic groups. The hydrophobic contours (Fig. 8a) show presence of three yellow(Y) contours at *ortho* and *para* position of the phenyl ring, in the

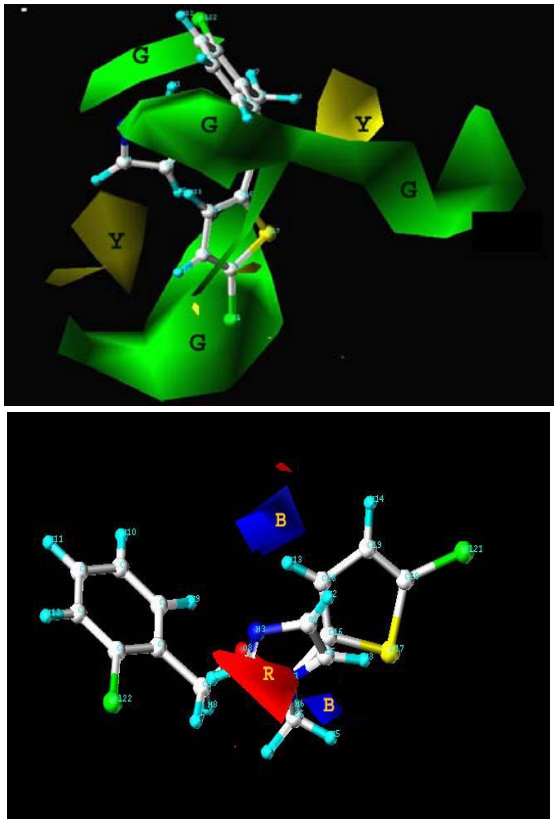

Fig. 7. The CoMSIA steric (a) and electrostatic (b) contour maps. One of the most active molecules **2** is shown in the background. Red (R) is a negative charged region, blue (B) a positively charged region, green (G) a positive sterically active region and yellow (G) a negatively sterically active region

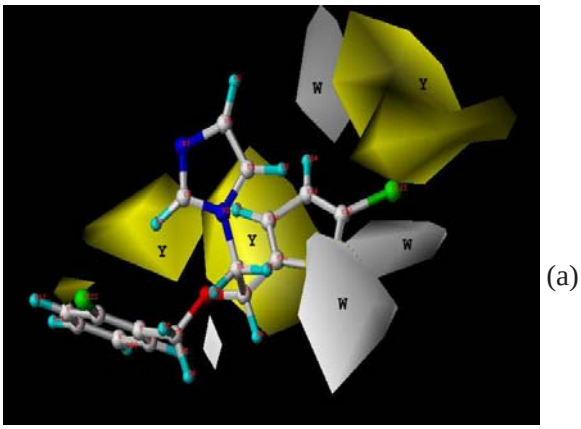

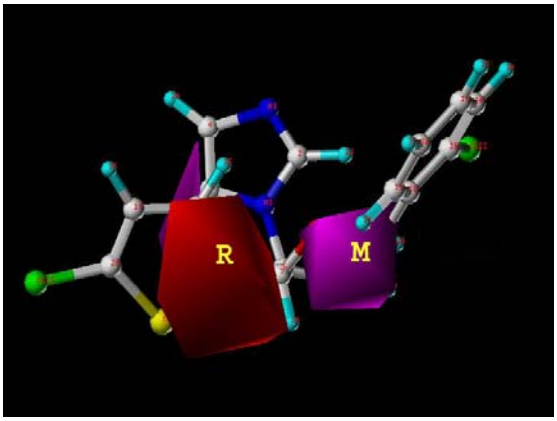

(b)

Fig. 8. The CoMSIA hydrophobic (a) and hydrogen bond acceptor (b) contour maps. One of the most active molecules **2** is shown in the background. Yellow (Y) is the hydrophobic region, white (W) hydrophilic region, magenta (M) a positively favoured hydrogen bond acceptor region and red (R) a negatively favoured active hydrogen bond acceptor region

linker (CH_2-CH) between the phenyl and the N1 of imidazole nucleus at the 2nd position of imidazole group where the hydrophobic substituents increase the activity. In hydrogen bond acceptor contours, the magenta (M) regions favour hydrogen bond acceptor groups while red(R) regions indicate unfavourable regions for acceptors. Two magenta (M) contours (Fig. 8b) are seen, at the ethereal linkage between the N1 of the imidazole and phenyl group and at the C4 and C5 of imidazole where the hydrogen bond acceptors may increase the activity. The CoMFA and CoMSIA models described are predictive enough to direct the design of new molecules.

Conclusion

The 3D-QSAR analyses, CoMFA and CoMSIA have been applied to a set of antifungal imidazoles active against *Candida albicans*. Statistically significant models with good correlative and predictive power for *Candida albicans* cytochrome $P450_{DM}$ inhibitory activities of the imidazole derivatives were obtained. However, it is evident from the predictive correlation coefficient that the CoMFA model was found to be superior to CoMSIA model inspite of the fact that CoMSIA has a combination of steric, electrostatic, hydrophobic and hydrogen bond acceptor fields. The results of this study may provide an important basis for future synthetic efforts in this area in that they offer useful suggestions about how to design new and more potent *Candida albicans* $P450_{DM}$ inhibitors.

ACKNOWLEDGEMENT

One of the authors (SB) gratefully acknowledges the financial support to this work by UGC in the form of Junior Research Fellowship.

REFERENCES

1. W.J. Watkins and T.E. Renau, Burger's Medicinal Chemistry and Drug Discovery, John Wiley and Sons. Inc., New Jersey, Vol. 5, edn. 6, p. 893 (2003).
2. R. Griffith and T. Tracy, Foye's Principles of Medicinal Chemistry, Lippincott Williams and Wilkins, Baltimore, edn. 5, p. 894 (2002).
3. A. Tafi, J. Anastassopoulou, T. Theophanides, M. Botta, F. Corelli, S. Massa, M. Artico, R. Costi, R.D. Santo and R. Ragno, *J. Med. Chem.*, **39**, 1227 (1996).
4. Y. Yoshida and Y. Aoyama, *J. Biol. Chem.*, **259**, 1655 (1984).
5. C.A. Hitchcock, K. Dickinson, S.B. Brown, E.G.V. Evans and D.J. Adams, *Biochem. J.*, **263**, 573 (1979).
6. J. Trazakos, S. Kawata and J.L. Gaylor, *J. Biol. Chem.*, **261**, 573 (1986).
7. H. Sono, Y. Sonoda and Y. Sato, *Biochim. Biophys. Acta*, **1078**, 388 (1984).
8. R.D. Cramer, D.E. Patterson and J.D. Bunce, *J. Am. Chem. Soc.*, **110**, 5959 (1988).
9. G.R. Desiraju, B. Gopalakrishnan, R.K. Jetti, A. Nagaraju, D. Raveendra, J.A. Sarma, M.E. Sobhia and R. Thilagavathi, *J. Med. Chem.*, **45**, 4847 (2002).
10. G.R. Desiraju, J.A. Sarma, D. Raveendra, B. Gopalakrishnan, R. Thilagavathi, M.E. Sobhia and H.S. Subramanya, *J. Phys. Org. Chem.*, **14**, 481 (2001).
11. A.K. Chakraborti, B. Gopalakrishnan, M.E. Sobhia and A. Malde, *Eur. J. Med. Chem.*, **38**, 975 (2003).
12. G. Klebe, U. Abraham and T. Mietzner, *J. Med. Chem.*, **37**, 4130 (1994).
13. SYBYL Molecular Modelling System, Version 7.1, Tripos Associates; St. Louis, MO.
14. E.F. Godefroi, J. Heeres, J.V. Cutsem and P.A.J. Janssen, *J. Med. Chem.*, **12**, 784 (1969).
15. J. Heeres, L.J. Backx and J.M. Van Cutsem, *J. Med. Chem.*, **19**, 1148 (1976).
16. M.T. Barakat and P.M. Dean, *J. Comput. Aided. Mol. Des.*, **4**, 295 (1990).
17. T. Halgren, *J. Am. Chem. Soc.*, **112**, 4710 (1990).
18. B.L. Podlogar and D.M. Ferguson, *Drug Des. Discov.*, **17**, 4 (2000).
19. M. Clark, R.D. Cramer, D.M. Jones, D.E. Patterson and P.E. Simeroth, *Tetrahedron Comput. Methodol.*, **3**, 47 (1990).

(*Received*: 7 August 2007; *Accepted*: 8 March 2008) AJC-6431